Narrowband Interference Avoidance for Ultra-Wideband Single-Carrier Block Transmissions with Frequency-Domain Equalization

Justin P. Coon, *Member, IEEE*

***Abstract*—In this article, a novel method of performing interference avoidance in next-generation single-carrier ultra-wideband block transmission systems is presented. This method relies on the application of a time-domain window to each data block prior to transmission, where the window is optimized such that the required notch depth is achieved for each transmission. Furthermore, a modification of this technique is also detailed, whereby the complexity can be reduced from $\mathcal{O}(N^3)$ to $\mathcal{O}(N^2)$ where N is the number of symbols per block. It is shown that the proposed techniques overcome many of the drawbacks of current methods such as transmit power control, frequency notching, and active interference cancellation.**

***Index Terms*—Ultra-wideband, interference avoidance, convex optimization, frequency-domain equalization, cognitive radio.**

I. Introduction

ULTRA-WIDEBAND (UWB) communication has become a popular (and controversial) topic [2]. The enormous capacity that is available at short distances has propelled UWB techniques to the forefront of cable replacement technology, with the first wireless universal serial bus (USB) devices scheduled to hit the market in the near future. A very attractive feature of UWB technology is that manufacturers are not required to pay license fees. Instead, UWB devices must transmit with a very low power spectral density (-41.3 dBm/MHz in the United States).

The lack of a licensing infrastructure for UWB systems has raised many questions by users and manufacturers that pay to use parts of the spectrum in the 3.1 GHz to 10.6 GHz band. Understandably, these parties are concerned that inexpensive UWB devices will flood the market and create a large amount of interference, which could cripple licensed systems. In an attempt to preempt this problem, several regulatory bodies have proposed that all UWB devices come equipped with an interference *detection and avoidance* (DAA) subsystem. The primary role of DAA algorithms is to first detect "interference" caused by a licensed user and then avoid corrupting that user's transmission. The idea of this type of DAA scheme is somewhat based on the principles of cognitive radio since DAA-equipped UWB devices would effectively transmit in an opportunistic manner (i.e. only when the licensed spectrum is free for use).

Manuscript received June 21, 2007; revised January 8, 2008 and May 7, 2008; accepted August 11, 2008. The associate editor coordinating the review of this paper and approving it for publication was X. Wang. This work was presented in part at WCNC 2007 [1].

J. P. Coon is with the Toshiba Telecommunications Research Laboratory, 32 Queen Square, Bristol (e-mail: justin.coon@toshiba-trel.com).

Digital Object Identifier 10.1109/T-WC.2008.070679

To date, several DAA approaches have been proposed for use in UWB systems. The "detection" part of DAA typically involves comparing the received power at a given frequency to a predetermined threshold to determine whether or not an interferer is present [3]. The "avoidance" part of DAA, which is the subject of this paper, generally proves to be more complicated. Crude methods of achieving interference avoidance include implementing transmit power control and/or frequency notching. Recently, however, several more sophisticated techniques have been studied. One such technique, proposed in [4] for use in multi-carrier CDMA systems, utilizes a particular type of spreading code to avoid interfering with licensed narrowband devices. By utilizing the same code to despread the message at the receiver, the narrowband interference is suppressed, which improves the overall performance of the system. A similar technique, known as *spectral encoding*, was documented in [5]. It should be noted that the techniques proposed in [4], [5] require both the transmitter and the receiver to have knowledge of the band in which the third-party device is transmitting *as well as* the spreading code that is employed in order to suppress the narrowband interference at the receiver.

In [6], an interference avoidance technique termed *active interference cancellation* (AIC) was proposed for use in orthogonal frequency division multiplexing (OFDM) systems. AIC relies on a combination of frequency notching (achieved through nulling subcarriers in an OFDM system) and intelligent tone excitation at the edges of the interference band. It has been shown that AIC can be used to create notches greater than 30 dB in depth [3], [6].

Recently, it has been proposed that next-generation UWB systems could be based on single-carrier block transmissions with frequency-domain equalization (SC-FDE) at the receiver (see, e.g., [7] for an overview of SC-FDE). DS-CDMA systems based on SC-FDE were proposed for UWB in [8]–[11]. In addition, more abstract SC-FDE systems were studied in the context of UWB channels in [12]–[15]. These works generally conclude that SC-FDE provides several advantages relative to an OFDM-based approach in UWB systems; however, they do not address the issue of interference avoidance in SC-FDE systems.

In this article, a novel approach to interference avoidance in SC-FDE systems is introduced. This approach relies on the application of a time-domain window to each data block prior to transmission. The window is optimized such that the required notch depth is achieved for each transmission.

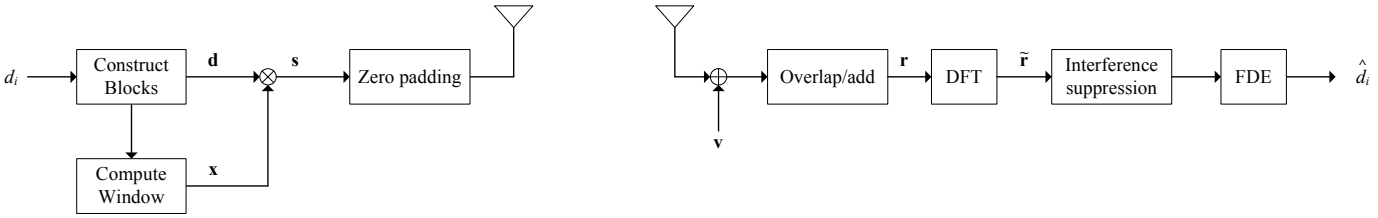

Fig. 1. Block diagram of a single-carrier block transmission system employing dynamic time-domain windowing to avoid interfering with narrowband transmissions.

Furthermore, the receiver is only required to have knowledge of the interference band in order to decode the received message, i.e., knowledge of the window used at the transmitter is not a prerequisite for decoding the received data. It should be noted that the detection of a narrowband interferer is a separate topic, and it is assumed throughout this paper that the UWB system is able to perfectly detect the presence of an interferer.

The paper is organized as follows. The system model is given in Section II. A method for computing the optimal time-domain window for interference avoidance is then detailed in Section III, and a reduced complexity variation of this algorithm is described in Section IV. Numerical results are presented in Section V, and conclusions are drawn in Section VI.

II. System Model with Window-aided Interference Avoidance

The interference avoidance approach that is proposed in this section is suitable for use in SC-FDE block transmission systems (see, e.g., [7]). The main idea of the proposed technique is to design a time-domain window that can be applied to a given data block at baseband such that the interference caused by the transmission in the band of interest is minimized. This approach is termed *window-aided interference avoidance* (WIA) in this paper. It should be noted that WIA is similar to the spectral encoding concept described in [5] in that it utilizes envelope scaling to create a notch in the desired part of the transmitted signal spectrum. However, spectral encoding requires the envelope scaling to be performed in the frequency domain — where a notch is created by ensuring the elements of the encoding sequence are '0' at the appropriate frequencies — whereas the method proposed here employs envelope scaling in the time domain.

Consider a system in which WIA is implemented (see Fig. 1). In this system, the information bits are encoded and interleaved, and subsequently mapped to (possibly) complex baseband constellation symbols. The baseband symbols $d[i]$ are parsed into blocks of length N, where the nth block is denoted by $\mathbf{d}_n := (d[nN], \ldots, d[N-1+nN])^T$. Each element of the data vector $\mathbf{d}_n \in \mathbb{C}^N$ is multiplied by the corresponding element of a window vector $\mathbf{x}_n \in \mathbb{R}^N$ to give

$$\mathbf{s}_n = \mathbf{D}_n \mathbf{x}_n \tag{1}$$

where $\mathbf{D}_n := \operatorname{diag}\{\mathbf{d}_n\}$. Redundancy in the form of N_P padded zeros is added to each precoded block[1], and the resulting sequence is used to modulate a train of pulses. The transmitted waveform can be represented as

$$\overline{s}(t) = \sum_{n=-\infty}^{\infty} \sum_{i=0}^{N-1} s[i+nN]\, p\left(t - (i+nN_G)\, T_s\right) \tag{2}$$

where $p(t)$ is the transmit pulse, $N_G = N + N_P$ is the total number of symbols in a block (including padded zero samples), and T_s is the symbol period.

Some UWB systems rely on a specific pulse shape to ensure that the transmission adheres to the spectral mask specified by the Federal Communications Commission (FCC). Typical pulse shapes that have been suggested in the literature include high-order Gaussian monocycle pulses and prolate spheroidal function-based pulses [16]. The method proposed here is applicable to any type of pulse since it operates in a baseband signal processing fashion; hence, only the baseband representation of the system is used for the remainder of the paper.

By applying the overlap-add technique to each length-N_G zero-padded block at the receiver, the linear convolution of the transmitted signal and the finite channel impulse response (CIR) becomes a circular convolution[2]. Thus, the nth baseband received block can be expressed as

$$\mathbf{r}_n = \boldsymbol{\mathcal{H}} \mathbf{s}_n + \mathbf{v}_n \tag{3}$$

where $\boldsymbol{\mathcal{H}} \in \mathbb{C}^{N \times N}$ is a circulant channel matrix, the first row of which is given by $(h_0, 0, \ldots, 0, h_L, \ldots, h_1)$; h_ℓ is the ℓth tap of the CIR; L is the memory order of the CIR; and $\mathbf{v}_n$ is a length-N vector of complex, zero-mean, white Gaussian noise samples with variance $\sigma_v^2/2$ per dimension. The vector $\mathbf{r}_n$ is transformed into the frequency domain to give $\tilde{\mathbf{r}}_n = \mathbf{F}\mathbf{r}_n$ where $\mathbf{F} \in \mathbb{C}^{N \times N}$ is the normalized discrete Fourier transform (DFT) matrix, the (k,m)th element of $\mathbf{F}$ being $F_{k,m} = N^{-1/2}\exp(-j2\pi km/N)$. Finally, a frequency-domain equalizer[3] and an inverse DFT are then applied to $\tilde{\mathbf{r}}_n$ to produce a time-domain estimate of the transmitted data block. Note that the techniques described in this paper operate on a block-by-block basis; consequently, the block index n is omitted from the following without loss of generality.

III. Computation of the Window

A. Problem Formulation

The objective is to define the window vector $\mathbf{x}$ such that the interference caused by the UWB signal on a given subset of

[1]Note that a cyclic prefix can be used in place of padded zeros, but only the latter is considered here for brevity.

[2]It should be noted that a considerable amount of research has been devoted to noncyclic single-carrier block transmission systems [17], [18]; however, the cyclic case is considered here for its facilitation of low-complexity FDE.

[3]Any linear or nonlinear frequency-domain equalizer can be used with the proposed technique (see, e.g., [7], [19], [20]).

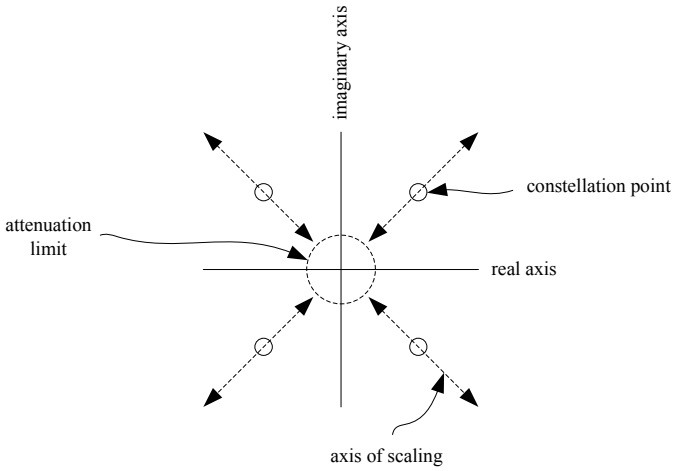

Fig. 2. Illustration of envelope scaling for QPSK.

frequency tones $\mathcal{I}$ is minimized. A group of discrete frequency tones is considered here instead of a portion of contiguous bandwidth because the single-carrier block transmission model resembles that of a multi-carrier system. Consequently, it will be sufficient to create a deep notch in the discrete sense as long as a suitable upsampling factor is used when computing the window.

Define the normalized upsampled DFT matrix as $\mathbf{W} \in \mathbb{C}^{\rho N \times N}$, where ρ is the sampling factor. The (k,m)th element of $\mathbf{W}$ is defined as $W_{k,m} = N^{-1/2}\exp(-j2\pi km/(\rho N))$. Now let $\mathbf{W}_{\mathcal{I}} \in \mathbb{C}^{Q \times N}$ denote the rows of $\mathbf{W}$ that correspond to the Q (upsampled) interference tones. Armed with this model, the vector $\mathbf{x}$ can be designed by taking a constrained optimization approach. In particular, the optimization problem can be stated as

$$\begin{array}{ll} \text{minimize} & \|\mathbf{W}_{\mathcal{I}}\mathbf{D}\mathbf{x}\|_2^2 \\ \text{subject to} & \|\mathbf{D}\mathbf{x}\|_2^2 = N \end{array}. \tag{4}$$

The vector $\mathbf{x}$ that minimizes (4) is easily found by using the method of Lagrange multipliers. In fact, the optimal vector $\mathbf{x}$ in this case is given by a Rayleigh quotient, and is simply an eigenvector of the interference-plus-data kernel. However, the elements of this vector can generally be either positive or negative real numbers. When the resulting window is applied to the corresponding data block, sign ambiguities arise, which must be resolved at the receiver in order to correctly decode the received message.

An additional constraint can be added to the original narrowband interference minimization problem stated above, which allows the receiver to perform detection and decoding without having knowledge of the window vector $\mathbf{x}$. In particular, the elements of $\mathbf{x}$ can be constrained to be greater than or equal to some nonnegative number δ. Furthermore, if the constellation that is used is limited to being a member of the set of constant-modulus constellations (e.g. QPSK), a simple nonnegative scaling of each data symbol would allow the receiver to distinguish between constellation points without knowledge of $\mathbf{x}$ (see Fig. 2). Under these constraints, and by relaxing the equality constraint in (4), the problem can be reformulated as

$$\begin{array}{ll} \text{minimize} & \|\mathbf{W}_{\mathcal{I}}\mathbf{D}\mathbf{x}\|_2^2 \\ \text{subject to} & \|\mathbf{x}\|_2^2 \le N \\ & \mathbf{x} \succeq \delta \mathbf{1}_N \end{array} \tag{5}$$

where $\mathbf{1}_N$ is a length-N column vector of ones. The problem stated in (5) is convex; thus, numerical nonlinear optimization methods, such as gradient descent methods and interior point methods [21], [22], can be employed to solve this problem efficiently. It should be noted that a similar approach to the one formulated above has been used to solve the problem of sidelobe suppression in OFDM systems [23].

TABLE I
BARRIER METHOD.

given strictly feasible $\mathbf{x}$, $t > 0$, $\mu > 1$, tolerance $\epsilon_o > 0$, and p constraints
repeat
1. compute the optimal vector $\mathbf{x}^\star(t)$ for the current value of t beginning at $\mathbf{x}$
2. $\mathbf{x} := \mathbf{x}^\star(t)$
3. quit if $p/t < \epsilon_o$
4. $t := \mu t$

B. Optimization Via the Barrier Method

The interior point method known as the barrier method is particularly suited to the constrained minimization problem stated above. The barrier method is summarized in Table I where p is the total number of constraints and μ is a step size [22]. In the barrier method, inequality constraints are added to the objective function by defining a logarithmic barrier constraint function for each inequality constraint [22]. In this case, there are $p = N + 1$ logarithmic barrier constraints, given by

$$g_1(\mathbf{x}) = -\frac{1}{t}\log\left(N - \|\mathbf{x}\|_2^2\right) \tag{6}$$

and

$$g_{m+1}(\mathbf{x}) = -\frac{1}{t}\log\left(\mathbf{e}_m^T\mathbf{x} - \delta\right) \tag{7}$$

where $\mathbf{e}_m$ is the mth length-N canonical unit column vector and the parameter t is the logarithmic barrier accuracy parameter [22]. These logarithmic constraint functions can be incorporated into the cost function to give the augmented cost function

$$f(\mathbf{x}) = tf_0(\mathbf{x}) + t\sum_k g_k(\mathbf{x}) \tag{8}$$

where $f_0(\mathbf{x}) := \|\mathbf{W}_{\mathcal{I}}\mathbf{D}\mathbf{x}\|_2^2$ is the original, unconstrained cost function.

Given a strictly feasible starting vector $\mathbf{x}$, the barrier method can be implemented as outlined in Table I to find the vector $\mathbf{x}$ that solves (5). With each iteration of the barrier method, a new "optimal" vector $\mathbf{x}^\star(t)$ must be computed by using one of any number of known optimization techniques. In particular, Newton's method — which is outlined in Table II — works well in this application [21], [22]. As an illustration of the effectiveness of WIA, Fig. 3 depicts the spectrum of a transmitted signal before and after the optimized window is applied. In this example, the data block comprised $N = 128$ BPSK symbols and the Newton-barrier method described above was used to find the (nearly) optimal window. The

TABLE II
NEWTON'S METHOD.

given a feasible starting point $\mathbf{x}$, tolerance $\epsilon_i > 0$
repeat
1. $\Delta\mathbf{x} = -\nabla^2 f(\mathbf{x})^{-1} \nabla f(\mathbf{x})$
   $\omega^2 = -\nabla f(\mathbf{x})^T \Delta\mathbf{x}$
2. quit if $\omega^2/2 < \epsilon_i$
   return $\mathbf{x}^\star := \mathbf{x}$
3. line search (determine θ)
4. $\mathbf{x} := \mathbf{x} + \theta\Delta\mathbf{x}$

shaded area in Fig. 3 represents the band in which the third-party narrowband signal resides.

C. Convergence Analysis - Self-concordance

The Newton-barrier algorithm presented above for performing dynamic spectral nulling in a single-carrier UWB block transmission system must be performed for each transmitted block. Consequently, it is logical to ask how fast the algorithm converges to an optimal window. Indeed, one might also inquire as to whether or not there are cases for which the algorithm does not converge at all. To answer these questions, a simple analysis based on self-concordance can be performed [22].

It is straightforward to show that the strictly convex composite cost function $f(\mathbf{x})$ is self-concordant, which implies that the Newton-barrier algorithm described above converges in all cases. Furthermore, the total number of Newton steps is bounded by [22]

$$N_t \leq \left\lceil \sqrt{p} \log_2 \frac{p}{t^{(0)}\epsilon_i} \right\rceil \left(\frac{1}{2\eta} + \log_2 \log_2 (1/\epsilon_i) \right) \quad (9)$$

where $t^{(0)}$ is the initial logarithmic barrier accuracy parameter, p is the number of constraints, ϵ_i is the specified accuracy of Newton's method (i.e. the measure of sub-optimality), α and β are strictly positive backtracking line search parameters, and

$$\eta = \frac{\alpha\beta(1-2\alpha)^2}{20-8\alpha}. \quad (10)$$

This bound is minimized for a given α and β where $0 < \alpha < 0.5$ and $0 < \beta < 1$ when

$$t^{(0)} \geq \frac{p}{\epsilon_i 2^{1/\sqrt{p}}} \quad (11)$$

in which case there is only one outer iteration in the Newton-barrier algorithm and the bound reduces to

$$N_t \leq \frac{1}{2\eta} + \log_2 \log_2 (1/\epsilon_i). \quad (12)$$

Furthermore, η is maximized when $\alpha \approx 0.1748$ and $\beta \approx 1$, in which case $1/2\eta \approx 126$ and

$$N_t \leq \log_2 \log_2 (1/\epsilon_i) + 126 \approx 129 \quad (13)$$

where the approximation is made for $\epsilon_i \approx 0.01$.

This simple analysis shows that the proposed algorithm will never require an excessively large number of Newton iterations to converge. However, it is important to note that the bound presented here is very loose. In fact, empirical studies show that the algorithm converges more than ten times faster in practice, after only 10.5 Newton iterations on average (with a standard deviation of approximately 1.1).

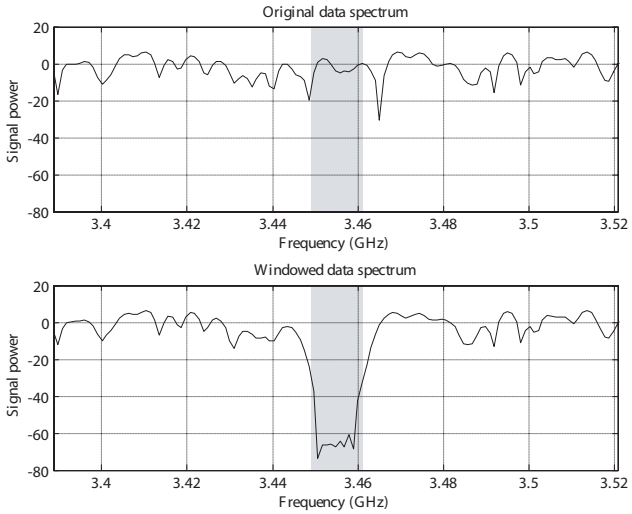

Fig. 3. Illustration of spectrum nulling via WIA. The shaded area represents the interference band.

IV. REDUCED-COMPLEXITY VARIATION

A. Algorithm

As indicated in Table I, the performance and complexity of the barrier method largely relies on the exact method that is used to compute the optimal vector $\mathbf{x}^\star(t)$. Although Newton's method works well, the inverse of the Hessian matrix of the augmented cost function must be computed with each iteration of the algorithm (cf. Table II), which can result in a high computational complexity when N is large. Fortunately, by reformulating the optimization problem given by (5), the complexity of the Newton-barrier method can be reduced from $\mathcal{O}(N^3)$ to $\mathcal{O}(N^2)$ as long as the signalling scheme is constrained to be BPSK or QPSK. Note that this restriction is inconsequential in wideband systems since these signalling schemes have been shown to be first-order optimal (and second-order optimal in the case of QPSK) in the wideband regime [24].

Consider the modified problem given by

$$\begin{array}{ll} \text{minimize} & \|\mathbf{W}_{\mathcal{I}}\mathbf{D}\mathbf{x}\|_2^2 \\ \text{subject to} & N - \epsilon \leq \|\mathbf{x}\|_2^2 \leq N + \epsilon \\ & \mathbf{x} \succeq \delta\mathbf{1}_N \end{array} \quad (14)$$

where the only differences between this problem and the one stated in (5) are the addition of a small tolerance[4] $\epsilon > 0$ to the norm constraint and the formulation of the box constraint. This modification ensures the power of the windowed signal will be very close to unity. Notice that since the box constraint is quadratic, the modified problem is not convex; nevertheless, this approach can be used to find a solution that is sufficient for most practical cases.

The general expression for the Hessian of the augmented objective function for the problem stated in (14) is given by

$$\nabla^2 f(\mathbf{x}) = t\nabla^2 f_0(\mathbf{x}) + t\sum_k \nabla^2 g_k(\mathbf{x}) \quad (15)$$

which is a function of both the optimization variable $\mathbf{x}$ and the diagonal data matrix $\mathbf{D}$. If either of these quantities changes,

[4]This should not be confused with the Newton-barrier accuracy parameters ϵ_o and ϵ_i in Tables I and II.

the Hessian and its inverse must be recomputed. However, the structure of the Hessian matrix can be exploited to reduce the complexity of each computation of the inverse of the Hessian matrix.

Through straightforward vector differentiation, it can be shown that the Hessians relating to the box inequality constraint are given by

$$\nabla^2 g_1(\mathbf{x}) = \frac{2}{t\Big(N-\epsilon-\|\mathbf{x}\|_2^2\Big)^2} \times \Big(2\mathbf{x}\mathbf{x}^T + \Big(N-\epsilon-\|\mathbf{x}\|_2^2\Big)\mathbf{I}_N\Big) \quad (16)$$

and

$$\nabla^2 g_2(\mathbf{x}) = \frac{2}{t\Big(N+\epsilon-\|\mathbf{x}\|_2^2\Big)^2} \times \Big(2\mathbf{x}\mathbf{x}^T + \Big(N+\epsilon-\|\mathbf{x}\|_2^2\Big)\mathbf{I}_N\Big). \quad (17)$$

Moreover, the sum of the Hessians corresponding to the lower bound on the elements of $\mathbf{x}$ in (14) is given by

$$\mathbf{\Lambda}(\mathbf{x}) := \sum_{k=3}^{p} \nabla^2 g_k(\mathbf{x}) = \operatorname{diag}\left\{\frac{1}{t\,(x_0-\delta)^2},\ldots,\frac{1}{t\,(x_{N-1}-\delta)^2}\right\}. \quad (18)$$

By assuming that $\|\mathbf{x}\|_2^2 \approx N$, which is reasonably accurate if $\epsilon \ll 1$, the first two expressions given above can be approximately written as

$$\nabla^2 \widetilde{g}_1(\mathbf{x}) = \frac{2}{t\epsilon^2}\big(2\mathbf{x}\mathbf{x}^T - \epsilon\mathbf{I}_N\big) \quad (19)$$

and

$$\nabla^2 \widetilde{g}_2(\mathbf{x}) = \frac{2}{t\epsilon^2}\big(2\mathbf{x}\mathbf{x}^T + \epsilon\mathbf{I}_N\big). \quad (20)$$

Furthermore, although the block power profile may fluctuate significantly about the mean, the matrix $\mathbf{\Lambda}(\mathbf{x})$ can be loosely approximated by

$$\widetilde{\mathbf{\Lambda}} = t\gamma\mathbf{I}_N, \quad \gamma \in \mathbb{R}_+. \quad (21)$$

The choice of the parameter γ is discussed further in the next subsection. Substituting these approximations into (15) gives

$$\nabla^2 f(\mathbf{x}) \approx \underbrace{2t\,\Re\mathfrak{e}\big\{\mathbf{D}^H\mathbf{W}_{\mathcal{I}}^H\mathbf{W}_{\mathcal{I}}\mathbf{D}\big\} + t\gamma\mathbf{I}_N}_{\mathbf{B}} + \frac{8}{\epsilon^2}\mathbf{x}\mathbf{x}^T \quad (22)$$

where the first term in (22) is the Hessian of $tf_0(\mathbf{x}) = t\,\|\mathbf{W}_{\mathcal{I}}\mathbf{D}\mathbf{x}\|_2^2$.

Notice that the first two terms on the right-hand side of (22) (the sum of which is denoted by the matrix $\mathbf{B}$) do not depend on the optimization vector $\mathbf{x}$, and the third term is a rank-one matrix. Rank-one updates to the inverse of a matrix are easily computed using $\mathcal{O}\big(N^2\big)$ complex multiplications via the matrix inversion lemma [25]; thus the inverse of the approximate Hessian matrix can be written as

$$\nabla^2 f(\mathbf{y})^{-1} \approx \mathbf{B}^{-1} - \frac{1}{1+\mathbf{y}^T\mathbf{B}^{-1}\mathbf{y}}\mathbf{B}^{-1}\mathbf{y}\mathbf{y}^T\mathbf{B}^{-1} \quad (23)$$

TABLE III
REDUCED-COMPLEXITY NUMERICAL ALGORITHM FOR INTERFERENCE AVOIDANCE.

given strictly feasible $\mathbf{x}$, $t>0$, $\tau>0$, $\gamma>0$, $\mu>1$,
tolerances $\epsilon_o, \epsilon_i > 0$, and p constraints
initialize $\mathbf{B}^{-1} = \frac{1}{\tau}\mathbf{D}^{-1}(\mathbf{\Omega}+\gamma\mathbf{I}_N)^{-1}\mathbf{D}^{-1}$
repeat
1. Newtons's method ($\mathbf{x}$, $\epsilon_i > 0$)
   a. **if** first iteration of Newton's method
      compute $\nabla^2 f(\mathbf{x})^{-1} = \mathbf{B}^{-1} - \frac{1}{\frac{\epsilon^2}{8}+\mathbf{x}^T\mathbf{B}^{-1}\mathbf{x}}\mathbf{B}^{-1}\mathbf{x}\mathbf{x}^T\mathbf{B}^{-1}$
   else
      proceed to step b.
   b. $\Delta\mathbf{x} = -\nabla^2 f(\mathbf{x})^{-1}\nabla f(\mathbf{x})$
      $\omega^2 = -\nabla f(\mathbf{x})^T\Delta\mathbf{x}$
   c. **if** $\omega^2/2 < \epsilon_i$
      or if notch depth is reached
      or if number of iterations exceeds $n_{max,i}$
      quit and return $\mathbf{x}^\star := \mathbf{x}$
   d. line search (determine β)
   e. $\mathbf{x} := \mathbf{x} + \beta\Delta\mathbf{x}$
2. $\mathbf{x} := \mathbf{x}^\star$
3. **if** $p/t < \epsilon_o$
   or if notch depth is reached
   or if number of iterations exceeds $n_{max,o}$
   quit
4. $t := \mu t$

where $\mathbf{y} := 2\sqrt{2}\,\epsilon^{-1}\mathbf{x}$. Consequently, the only direct matrix inverse that must be computed is $\mathbf{B}^{-1}$.

Now let the signalling scheme be restricted to BPSK, in which case $\mathbf{D}^H = \mathbf{D}^T = \mathbf{D}$ and

$$\mathbf{B} = t\,(\mathbf{D}\mathbf{\Omega}\mathbf{D} + \gamma\mathbf{I}_N) \quad (24)$$

where $\mathbf{\Omega} := 2\,\Re\mathfrak{e}\big\{\mathbf{W}_{\mathcal{I}}^H\mathbf{W}_{\mathcal{I}}\big\}$. It follows that

$$\mathbf{B}^{-1} = \frac{1}{t}\mathbf{D}^{-1}(\mathbf{\Omega}+\gamma\mathbf{I}_N)^{-1}\mathbf{D}^{-1} \quad (25)$$

which can be partly precomputed for given interference bands, leaving only the pre- and postmultiplication by the diagonal matrix $\mathbf{D}^{-1}$ once per data block and scaling by $1/t$ for each outer iteration of the barrier method. Fixing t at some predetermined value $t=\tau$ can reduce the complexity even further, resulting in the computation of $\mathbf{B}^{-1}$ once per data block (at the beginning of the first iteration of the barrier method).

Note that QPSK signalling can be supported by performing the steps outlined above for both the in-phase and the quadrature components separately. Higher-order signalling schemes can be supported in a similar manner; in this case, however, signal separation techniques such as interleave division multiple access (IDMA) [26] must be used to recover the transmitted message at the receiver.

The approach outlined above is summarized in Table III, where the parameters $n_{max,i}$ and $n_{max,o}$ are the specified maximum allowable numbers of Newton iterations and barrier iterations, respectively. These limits are required in practice since unbounded or variable-length iterative algorithms are difficult to implement in hardware.

B. Complexity and Convergence

Since the problem stated in (14) is nonconvex, a traditional convergence analysis based on the self-concordance of the

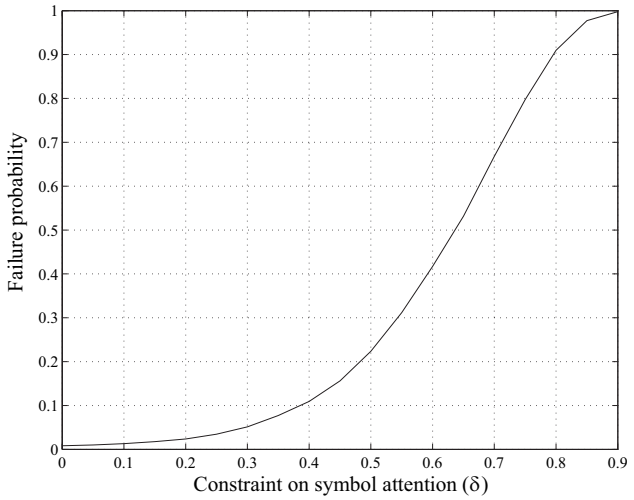

Fig. 4. The probability that a windowed transmission fails to meet the required depth in the interference band without the use of transmit power control illustrated as a function of the attenuation constraint δ.

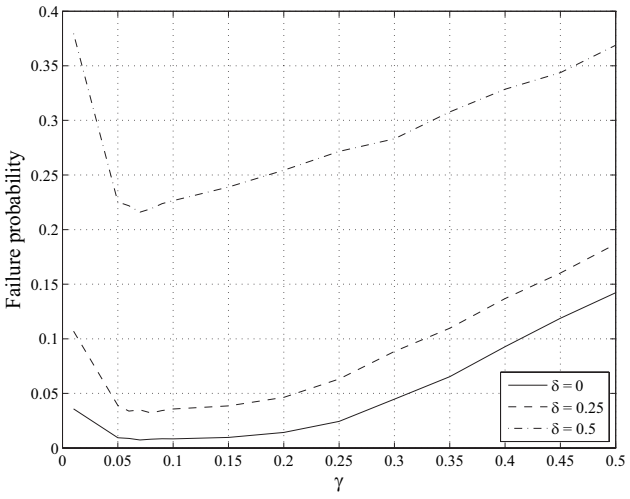

Fig. 5. The probability that a windowed transmission fails to meet the required depth in the interference band without the use of transmit power control illustrated as a function of the parameter γ for $\tau = 100$ and $\delta = 0, 0.25$, and 0.5.

augmented objective function cannot be performed. Furthermore, the addition of multiple stopping criteria (see Table III) makes analyzing the convergence of the reduced-complexity algorithm very difficult. However, empirical results show that approximately 24 Newton iterations are required on average to achieve a notch depth of -30 dB (with a standard deviation of approximately 10 iterations). Although the modified algorithm presented here clearly shows worse convergence than the convex Newton-barrier algorithm discussed in Section III, the complexity of the modified algorithm is still significantly less than the convex program due to the approximations that are made when computing the inverse of the Hessian matrix.

C. Choice of the Attenuation Limit δ

It is beneficial to choose a parameter δ that provides sufficient flexibility for deep frequency notch creation while facilitating robust blind detection at the receiver. If δ is chosen to be small, some data symbols may not be transmitted with much power, which leads to a lower SNR for those symbols at the receiver. Consequently, the overall performance of the system will suffer[5]. Alternatively, by choosing a high value of δ, the degradation in bit error rate (BER) due to windowing can be minimized; however, in this case, the proposed WIA algorithms tend to converge slowly or not at all in the sense that the specified notch depth cannot be met.

In practice, transmit power control must be employed when the target notch depth is not met. Consequently, it is interesting to study the probability that a *notch failure* occurs. This is illustrated in Fig. 4 for the reduced-complexity algorithm detailed in Section IV-A. In this analysis, a *failure* is defined as the event where the proposed technique fails to achieve a notch depth of -71.3 dBm/MHz – which is 30 dB/MHz below the spectral mask specified by the FCC for UWB transmissions – after 30 iterations of the Newton-barrier method ($n_{max,i} = 10$ and $n_{max,o} = 3$). It is clear from this figure that a low attenuation constraint is beneficial in terms of algorithm convergence.

[5]See [23] for an analysis of the bit error rate for windowed OFDM systems.

D. Choice of the Parameters τ and γ

Careful consideration should be taken when choosing the parameters γ and τ. Since the product $\tau\gamma$ approximates $(x_k - \delta)^{-2}$ for all k in the approximate Hessian $\tilde{\mathbf{\Lambda}} = \tau\gamma\mathbf{I}_N$, it stands to reason that this product should be chosen to be on the order of $E\left\{(x_m - \delta)^{-2}\right\}$. However, one must also consider the effect that τ has on the total approximate Hessian matrix. If τ is too small, very little emphasis will be placed on the accuracy of the Hessian matrix (since τ is just an instantiation of the logarithmic accuracy parameter t), whereas if τ is too large, the convergence of the algorithm will suffer.

Fig. 5 depicts the failure probability (as defined above) as a function of γ for $\tau = 100$ and $\delta = 0, 0.25$, and 0.5. Note that this choice of τ was found to provide a good trade-off between the convergence of the algorithm and the accuracy of the Hessian approximation. Interestingly, it is observed in this example that a low failure probability is achieved if $\gamma \in [0.05, 0.15]$ with the optimal value being $\gamma \approx 0.075$, or equivalently $\tau\gamma = 7.5$. This result supports the previously stated hypothesis that τ and γ should be chosen such that $\tau\gamma$ is on the order of $E\left\{(x_m - \delta)^{-2}\right\}$.

V. Results and Discussion

In this section, properties of the transmitted WIA signal, such as dynamic range and peak-to-average power ratio (PAPR), are investigated. Furthermore, the performance of a system employing this technique is studied in terms of packet error rate (PER).

A. Dynamic Range and Peak-to-average Power Ratio

A clear drawback of the proposed technique is that the time-varying fluctuations in signal power due to the application of the window will lead to an increase in the dynamic range of the transmitted signal. Each window vector $\mathbf{x}$ is a function of a given data block, and all windows are independent of each other. Consequently, a logical way to measure the dynamic range of the signal is by observing the statistical standard

TABLE IV
STANDARD DEVIATION OF WINDOW COEFFICIENTS (99TH PERCENTILE).

δ	Standard deviation
0	0.37
0.25	0.37
0.5	0.35
0.75	0.26

deviation of the window coefficients on a block-by-block basis. In this way, a *percentile* standard deviation can be calculated. The 99th percentile standard deviations for various attenuation limits δ are outlined in Table IV. For example, it is observed in this table that 99% of windows computed with an attenuation limit of $\delta = 0$ have coefficients with a standard deviation less than 0.37. Moreover, it is clear from these results that if WIA is employed with low resolution fixed-point arithmetic, it is beneficial to choose the attenuation limit δ to be high (e.g., $\delta = 0.75$).

Another property of the transmitted signal that must be quantified is its PAPR. While conventional single-carrier modulation benefits from an inherently low PAPR, the application of a window to each data block will clearly lead to an increase in the peak power of the transmitted signal. Fig. 6 illustrates the complementary cumulative distribution functions (CCDFs) of the PAPR for various attenuation limits. To generate this figure, an ensemble of single-carrier data blocks were randomly generated and a window was computed and applied to each one (except for the reference case). The resulting blocks were filtered with a raised cosine filter with a roll-off factor of 0.5. It is observed in this figure that the windowing operation degrades the PAPR of the signal by several dB. However, the resulting PAPR is still less than that of an OFDM signal, especially for the cases where $\delta = 0$ and $\delta = 0.75$.

B. Packet Error Rate

The PER of SC-FDE systems that employ WIA with $\delta = 0, 0.25, 0.5,$ and 0.75 are plotted against distance[6] in Fig. 7. Furthermore, the performance of a system that utilizes the AIC method proposed in [6], which was adapted for use with single-carrier transmissions, without full knowledge of the location of the interference band is shown. As a reference, the PER of an SC-FDE system where no interference avoidance techniques are implemented (or required) is illustrated.

In these simulations, 1024 bits (including tail bits) were encoded with a half-rate convolutional code defined by the octal code polynomials $(133)_8$ and $(171)_8$. The encoded bits were interleaved before being mapped to BPSK symbols. These symbols were arranged into blocks of length $N = 128$, and the optimized envelope was computed for the WIA systems by using the algorithm described in Section IV. The Newton-barrier method was allowed to run for a maximum of 30 iterations ($n_{max,i} = 10$ and $n_{max,o} = 3$) for each envelope computation, and the target notch depth of -71.3 dBm/MHz was met in most cases for $\delta = 0$ and 0.25 (cf. Fig. 4). Each envelope was applied to its corresponding data block, and groups of two successive blocks were superimposed using the in-phase/quadrature approach described in Section IV prior to transmission. The data was transmitted in the 3.1 GHz to 3.6 GHz band, and the notch was created over a bandwidth of 12 MHz. The link budget parameters specified in [27] were used along with the IEEE 802.15.4a UWB channel model for a line-of-sight (LOS) office environment [28] to simulate the wireless channel and compute the SNR for a given distance. A linear MMSE frequency-domain equalizer was used to equalize the signal at the receiver.

[6]Distance, as opposed to received SNR, is often used when characterizing the performance of UWB systems due to the strict transmit power spectral density of -41.3 dBm/MHz that the FCC has placed on UWB transmissions.

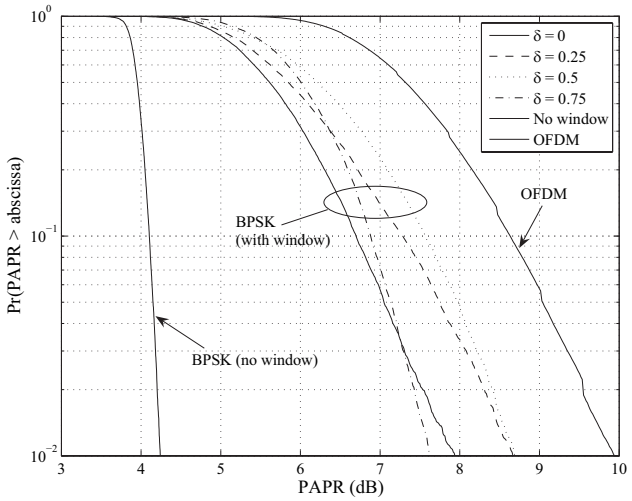

Fig. 6. CCDF of PAPR for single-carrier systems with $\delta = 0, 0.25, 0.5,$ and 0.75.

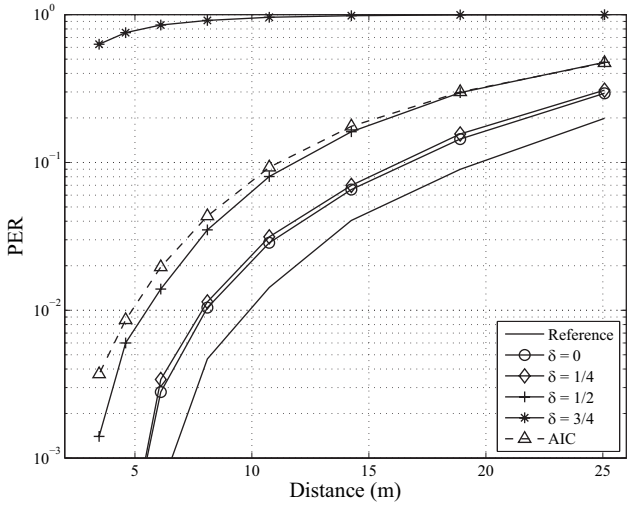

Fig. 7. Packet error rate vs. distance for single-carrier systems with $\delta = 0, 0.25, 0.5,$ and 0.75.

The example in Fig. 7 shows the effectiveness of the proposed technique for low values of δ when a strict limitation is placed on the number of iterations. This limitation ensures that the complexities of the systems that employ WIA are similar. Thus, although a system that uses WIA with $\delta = 0.25$ performs significantly better than one where $\delta = 0.5$, this advantage *does not* come at the cost of an increased complexity. Instead, the performance advantage can be attributed to the high failure probability of the WIA algorithm when $\delta = 0.5$ as discussed in Section IV-C.

Finally, note that the system that utilizes AIC performs much worse than the proposed system for $\delta = 0$ and $\delta = 0.25$.

In this case, however, the advantage of the WIA approach *does* come at the cost of greater complexity. In particular, the complexity of AIC is $\mathcal{O}\left(T^3\right)$ where T denotes the number of interference tones (i.e., the number of subcarriers in the notch). In contrast, the complexity of the proposed windowing method is $\mathcal{O}\left(N^2\right)$ as mentioned in Section IV. Consequently, the AIC technique is considerably less complex than the proposed method for narrow notches. However, this advantage diminishes quickly as the required notch depth increases.

VI. Conclusions

Narrowband interference detection and avoidance is an essential part in cognitive radio, and is an important issue that must be addressed in future UWB systems. In this paper, a novel approach to performing interference avoidance was presented. This approach relies on the application of a dynamic time-domain window to each data block prior to transmission. In particular, it was shown that the window can be computed by formulating a convex optimization problem, which was shown to converge in only a few iterations of the algorithm. This technique can suffer from a high computational complexity. As a result, a reduced complexity implementation was also presented. Both methods utilize windows with real-valued, positive coefficients, which facilitates the reliable decoding of the received message without the need for side information when constant-modulus constellations are used. It was shown through simulations that the PER of a system that employs the proposed algorithm performs significantly better than a system where AIC is employed when neither system has perfect knowledge of the interference band.

Acknowledgment

The author would like to thank Dr. D. McNamara and Dr. S. Parker of Toshiba Research Europe Ltd. (TREL) as well as the anonymous reviewers for their suggestions in preparing this work. The author would also like to acknowledge the support of the directors at TREL.

References

[1] J. P. Coon, "Optimization of single-carrier UWB transmissions for narrowband interference avoidance," in *Proc. IEEE Wireless Commun. and Networking Conference (WCNC)*, Mar. 2007.

[2] S. Roy, J. R. Foerster, V. S. Somayazulu, and D. G. Leeper, "Ultrawideband radio design: the promise of high-speed, short-range wireless connectivity," *Proc. IEEE*, vol. 92, no. 2, pp. 295–311, Feb. 2004.

[3] S. Shetty, "Detect and avoid (DAA) techniques - enabler for worldwide ultrawideband regulations," Staccato Communications, Tech. Rep., May 2006. [Online]. Available: http://www.iee.org/Events/Shetty.pdf

[4] P. Yaddanapudi and D. C. Popescu, "Narrowband interference avoidance in ultra wideband communication systems," in *Proc. IEEE Global Telecommun. Conference (Globecom)*, vol. 6, Nov. 2005, pp. 3779–3783.

[5] C. R. C. M. da Silva and L. B. Milstein, "Spectral-encoded UWB communication systems: real-time implementation and interference suppression," *IEEE Trans. Commun.*, vol. 53, no. 8, pp. 1391–1401, Aug. 2005.

[6] H. Yamaguchi, "Active interference cancellation technique for MB-OFDM cognitive radio," in *Proc. Microwave Conference, 2004. 34th European*, vol. 2, Oct. 13, 2004, pp. 1105–1108.

[7] D. Falconer, S. L. Ariyavisitakul, A. Benyamin-Seeyar, and B. Eidson, "Frequency domain equalization for single-carrier broadband wireless systems," *IEEE Commun. Mag.*, vol. 40, no. 4, pp. 58–66, Apr. 2002.

[8] Y. Ishiyama and T. Ohtsuki, "Performance evaluation of UWB-IR and DS-UWB with MMSE-frequency domain equalization (FDE)," in *Proc. IEEE Global Telecommun. Conference (Globecom)*, vol. 5, Nov. 2004, pp. 3093–3097.

[9] H. Sato and T. Ohtsuki, "Performance evaluation of frequency domain equalization and channel estimation for direct sequence-ultra wideband (DS-UWB) system," in *Proc. IEEE Vehicular Technology Conference (VTC)*, vol. 1, May 2005, pp. 481–485.

[10] S. Yoshida, T. Ohtsuki, and T. Kaneko, "Improvement of bandwidth efficiency of UWB-IR and DS-UWB with frequency-domain equalization (FDE) based on cyclic prefix (CP) reconstruction," in *Proc. IEEE Vehicular Technology Conference (VTC)*, vol. 2, Sep. 2005, pp. 991–995.

[11] H. Sato and T. Ohtsuki, "Frequency domain channel estimation and equalisation for direct sequence ultra wideband (DS-UWB) system," *IEE Proc. Commun.*, vol. 153, pp. 93–98, Feb. 2, 2006.

[12] Y. Wang and X. Dong, "Performance of SC-FDE in UWB communications with channel estimation errors," in *Proc. IEEE Pacific Rim Conference on Communications, Computers and signal Processing (PACRIM)*, Aug. 2005, pp. 21–24.

[13] Y. Wang, X. Dong, P. H. Wittke, and S. Mo, "Cyclic prefixed single carrier transmission in ultra-wideband communications," in *Proc. IEEE International Conference on Commun. (ICC)*, vol. 4, May 2005, pp. 2862–2866.

[14] Y. Wang and X. Dong, "A time-division multiple-access SC-FDE system with IBI suppression for UWB communications," *IEEE J. Select. Areas Commun.*, vol. 24, no. 4, pp. 920–926, Apr. 2006.

[15] Y. Wang, X. Dong, P. H. Wittke, and S. Mo, "Cyclic prefixed single carrier transmission in ultra-wideband communications," *IEEE Trans. Wireless Commun.*, vol. 5, no. 8, pp. 2017–2021, Aug. 2006.

[16] B. Hu and N. C. Beaulieu, "Pulse shapes for ultrawideband communication systems," *IEEE Trans. Wireless Commun.*, vol. 4, no. 4, pp. 1789–1797, July 2005.

[17] Z. Wang, X. Ma, and G. B. Giannakis, "OFDM or single-carrier block transmissions?" *IEEE Trans. Commun.*, vol. 52, no. 3, pp. 380–394, Mar. 2004.

[18] Z. Wang and G. B. Giannakis, "Wireless multicarrier communications: Where Fourier meets Shannon," *IEEE Signal Processing Mag.*, vol. 17, no. 3, pp. 29–48, May 2000.

[19] M. V. Clark, "Adaptive frequency-domain equalization and diversity combining for broadband wireless communications," *IEEE J. Select. Areas Commun.*, vol. 16, no. 8, pp. 1385–1395, Oct. 1998.

[20] N. Benvenuto and S. Tomasin, "On the comparison between OFDM and single carrier modulation with a DFE using a frequency-domain feedforward filter," *IEEE Trans. Commun.*, vol. 50, no. 6, pp. 947–955, June 2002.

[21] R. Fletcher, *Practical Methods of Optimization*, 2nd ed. Wiley, 1987.

[22] S. Boyd and L. Vandenberghe, *Convex Optimization*. Cambridge University Press, Mar. 2004.

[23] I. Cosovic, S. Brandes, and M. Schnell, "Subcarrier weighting: a method for sidelobe suppression in OFDM systems," *IEEE Commun. Lett.*, vol. 10, no. 6, pp. 444–446, June 2006.

[24] S. Verdú, "Spectral efficiency in the wideband regime," *IEEE Trans. Inform. Theory*, vol. 48, no. 6, pp. 1319–1343, June 2002.

[25] T. K. Moon and W. C. Stirling, *Mathematical Methods and Algorithms for Signal Processing*. Prentice Hall, 2000.

[26] H. Schoeneich and P. A. Hoeher, "Adaptive interleave-division multiple access A potential air interface for 4G bearer services and wireless LANs," in *Proc. First IFIP International Conference on Wireless and Optical Commun. Networks (WOCN)*, June 2004, pp. 179–182.

[27] A. Batra, J. Balakrishnan, G. R. Aiello, J. R. Foerster, and A. Dabak, "Design of a multiband OFDM system for realistic UWB channel environments," *IEEE Trans. Microw. Theory Technol.*, vol. 52, pp. 2123–2138, Sept. 2004.

[28] A. F. Molisch, D. Cassioli, C.-C. Chong, S. Emami, A. Fort, B. Kannan, J. Karedal, J. Kunisch, H. G. Schantz, K. Siwiak, and M. Z. Win, "A comprehensive standardized model for ultrawideband propagation channels," *IEEE Trans. Antennas Propag.*, vol. 54, no. 11, pp. 3151–3166, Nov. 2006.

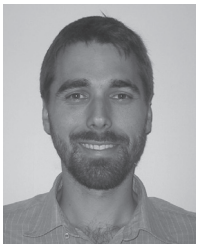

Justin P. Coon received the B.S. degree (with distinction) in electrical engineering from the Calhoun Honors College at Clemson University, South Carolina, in December 2000, and the Ph.D. degree in wireless communications from the University of Bristol, England, in 2005. At present, he is a Senior Research Engineer with Toshiba Research Europe's Telecommunications Research Laboratory in Bristol. He is also an Editor for the IEEE Transactions on Wireless Communications. Dr. Coon's current research interests include communication theory, wideband communications, and multiple-antenna systems.